ENGINEERING TRANSACTIONS • *Engng. Trans.* • **49**, 4, 485–510, 2001
Polish Academy of Sciences • Institute of Fundamental Technological Research
10.24423/engtrans.539.2001

DIRECT STIFFNESS ENERGY MODEL FOR A ONE-DIMENSIONAL COMPLEX SYSTEM

M. N. ICHCHOU and L. JEZEQUEL

Laboratoire de Tribologie et Dynamique des Systèmes
École Centrale de Lyon
36, Avenue Guy de Collongue 69131 BP 163 Écully FRANCE
e-mail: ichchou@mecasola.ec-lyon.fr

This paper deals with the high frequency analysis of one-dimensional waveguides. In this frequency range, this paper proposes a numerical implementation and tests of an alternative to the classical predictive dynamical methods. The originality of this approach consists in the fact that it is solely an energy density description. A numerical scheme very similar to the well-known direct stiffness method is employed here. This leads to a numerical code capable of predicting the mean value energy density for complex beam-like structure up to high frequencies. A twenty-four components plane truss, including both the bending and extension motion is used as a verification test, and shows the ability of the proposed code to predict the high frequency dynamics of complex beam-like structures.

1. INTRODUCTION

The medium and high frequency dynamics is the subject of intensive research and a great number of works and publications confirms the interest of the scientific community in such questions. In fact, there is still a real need for inventing methods well suited to deal with medium and high frequencies and taking into account the numerous problems of this domain. These problems make the use of the classical methods (finite element, boundary element,...) not always possible, for many reasons to be discussed below.

Among the classical methods which are widely employed in the prediction of sound and vibration level of industrial machines, let us mention the finite element method as an example. From a global point of view, this method based on the Rayleigh scheme uses a discretisation procedure which is mainly dependent on the complexity of the studied cases and of the frequencies of interest. Indeed, as the frequency increases, the wavelength decreases and a great number of elements

are needed. This leads to difficulties in the numerical analysis. Moreover, in the strict analysis of the features of high frequencies, it should be noticed that the main argument against the use of classical methods is the damping phenomenon which has a leading role. In fact, as the frequency increases, the modes are strongly coupled whilst the approximation of the dynamical behavior by finite element method advances the superposition of the uncoupled modes.

In the light of this succinct description, the development of further possibilities appears to be necessary. Among them, let us mention the well known *Statistical Energy Analysis* (SEA). This method appeared in early seventies. The (SEA) proposes an analysis of the energy transfer between subsystems (set of modes). From a (SEA) scheme, a global tendency of the total energy is then given. Nevertheless, the (SEA) needs to be improved in order to avoid its deficiencies. The reader can, in this context, be referred to the review of the *Statistical Energy Analysis* [1], where an interesting survey and a number of critical comments are given.

Owing to the exposed literature survey, a number of works appeared to enhance the *Statistical Energy Analysis* robustness and productivity. Among those attempts let us report the earlier work of BELOV and RYBAK [2] and the interesting investigations of NEFSKE and SUNG [3], who proposed the use of the heat conduction analogy to get not only the total energy available in a (SEA) model, but also the space evolution of energy density within the subsystems. This leads to energy formulation of the dynamical equation of motion instead of the classical displacement-based model. This model has been improved by BERNHARD and his team [4 – 7] and studied also by ICHCHOU, LE BOT and JEZEQUEL [8 – 12].

The main goal of this paper is to present a numerical implementation of such a technique in order to build an energy code. In fact, we first shortly present the basis of the technique and a general formulation needed to couple the subsystems. The *Direct Stiffness Method* is used to solve the energy equation and to implement the method. A verification test is finally considered. The latter is a complex plane lattice comprising twenty four bar elements. This example has been chosen since it has been treated by other contributors in the literature using different approaches to the problem [13, 14].

2. A BRIEF REVIEW OF THE LOCAL ENERGY EQUATION

This section attempts to summarize the main definitions and steps needed in order to understand the energy equation properties. Accordingly, in the subsequent presentation, the term w_α will denote a propagating plane wave (of the kind defined by index α) in a one-dimensional medium (Fig. 1). Precisely, it will designate a bending, extension or torsion plane wave propagating in a bar

element. However, the presentation is suited for a more general case. Moreover, when needed, an evanescent wave will be indicated by the term ϵ_α (see Fig. 1). Note that both the phase and the amplitude are included in the notation used here *(complex notation is then implicit)*. Finally, let us mention that only steady

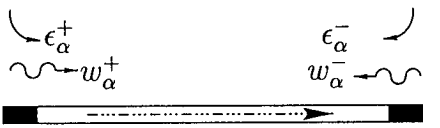

FIG. 1. Wave designation into a simple wave guide

state dynamics will be taken into account below, ω representing angular velocity of propagating wave. Therefore, no transient aspect is involved in this study. Let us also denote by "s" the identifying mark on the neutral axis of the bar. On the basis of the energy equation formulation, two **continuous** energy parameters are introduced. The first energy quantity is nothing else but the total energy density $W(s)$ defined as the sum of the potential energy density and the kinetic energy density. The second energy variable $I(s)$ is the active energy flow defined as the real part of the complex energy flow. These parameters are continuous, contrary to (SEA), where such parameters are discreetes. The quantities introduced in the framework of this model may be related to classical energy quantities deduced from motion equations by various ways. The common idea of all these interpretations is that the energies considered here are classical energies where all irrelevant details in a high frequency view are removed. Usually, local averages over time, space, frequency or ensemble are involved.

Consider now the simplest waveguide, where two travelling waves exist: an incident propagating wave (*incoming*) denoted w_α^+, and a reflected (or *outgoing*) travelling wave denoted w_α^-. Far from singularities, only *pure propagative waves are kept.* In fact, evanescent waves are mainly concentrated at the junctions or sources locations, and they will not contribute to the dynamics far from those locations. It is the first hypothesis of the energy equation. Then, partial energy quantities can be introduced and defined as the energy variables associated with each kind of travelling waves. I_α^+, I_α^-, W_α^+ and W_α^- will represent respectively the active energy flow and the energy denity associated with the incident and reflected progressive waves. To close the preliminary presentation, a set of required parameters may be described. Those parameters are: the group velocity c_{g_α}, and the characteristic impedance Z_α associated with the system. It can be readily shown that partial energy flow quantities can be related to the associated waves by the general relationship (2.1):

$$I_\alpha^+ = \frac{1}{2}\omega^2 Z_\alpha w_\alpha^+ \bar{w}_\alpha^+, \qquad I_\alpha^- = -\frac{1}{2}\omega^2 Z_\alpha w_\alpha^- \bar{w}_\alpha^-. \tag{2.1}$$

In order to establish a relationship between the partial and global energy parameters, another assumption is introduced. This assumption postulates that waves interferences are not considered in the formulation of the model. As a consequence, a superposition principle can be employed for the quadratic parameter as it is the case for displacement parameters. Hence, this assumption leads to (2.2):

$$W_\alpha(s) = W_\alpha^+(s) + W_\alpha^-(s), \quad I_\alpha(s) = I_\alpha^+(s) - I_\alpha^-(s). \tag{2.2}$$

The first step in deriving the energy equation is the local energy balance for a non-loaded region:

$$\text{div}.I_\alpha + p_{\alpha_{\text{diss}}} = 0, \tag{2.3}$$

where $p_{\alpha_{\text{diss}}}$ is the power density being dissipated. The damping model adopted here is the same as in (SEA): power density being dissipated is proportional to the energy density. Hence:

$$p_{\alpha_{\text{diss}}} = \eta_\alpha \omega W_\alpha, \tag{2.4}$$

where η_α is the damping loss factor. The validity of this relationship has been discussed in the literature concerning (SEA). As the travelling wave is a particular solution of the motion equation, the power balance (2.3) may be applied and leads to:

$$\frac{dI_\alpha}{ds}^{\pm} + p_{\alpha_{\text{diss}}}^{\pm} = 0. \tag{2.5}$$

As we are concerned with pure travelling waves, a simple relationship exists between partial energy flow and partial energy density [15]:

$$I_\alpha{}^{\pm}(s) = \pm c_{g_\alpha} W_\alpha^{\pm}(s). \tag{2.6}$$

The minus sign, before the group velocity, stems from the direction of propagation. The power densities being dissipated are given, as in (SEA), by:

$$p_{\alpha_{\text{diss}}}^{\pm} = \eta_\alpha \omega W_\alpha^{\pm}. \tag{2.7}$$

Now, substituting (2.7), (2.6) in the power balance relationship (2.5), we obtain:

$$I_\alpha^{\pm}(s) = \frac{-c_{g_\alpha}^2}{\eta_\alpha \omega} \frac{dW_\alpha}{ds}^{\pm}. \tag{2.8}$$

Adding equations (2.8), a relationship between $I_\alpha(s)$ and $W_\alpha(s)$ is obtained:

$$I_\alpha(s) = \frac{-c_{g_\alpha}^2}{\eta_\alpha \omega} \frac{dW_\alpha}{ds}, \tag{2.9}$$

which is similar to the thermal conductivity law (2.9). Finally, introducing this relationship into the power balance, we obtain:

$$\frac{d^2 W_\alpha}{ds^2} - \left(\frac{\eta_\alpha \omega}{c_{g_\alpha}}\right)^2 W_\alpha(s) = 0. \tag{2.10}$$

Equation (2.10) is analogous to the steady state heat conduction equation with a convective term. The solutions of this equation exhibit a slow space evolution, contrary to the energy densities predicted from the classical governing equations. The energy equation (2.10) predicts only the macroscopic evolution of the energy density, without any details of the smallest oscillation which are not relevant for the medium and high-frequency models. This is the sense of the local space average introduced in [4]. Alternatively, the solution of this energy equation may be viewed as the space or frequency average of the energy density deduced from the classical governing equations. As a compensation for this lack of information, a significant gain is obtained in the time-computation up to high frequencies. General solution of this equation is:

$$W_\alpha(s) = A_\alpha^+ e^{-\frac{\eta_\alpha \omega}{c_{g_\alpha}} s} + A_\alpha^- e^{\frac{\eta_\alpha \omega}{c_{g_\alpha}} s}, \tag{2.11}$$

for the energy density, and:

$$I_\alpha(s) = c_{g_\alpha} \left[A_\alpha^+ e^{-\frac{\eta_\alpha \omega}{c_{g_\alpha}} s} - A_\alpha^- e^{\frac{\eta_\alpha \omega}{c_{g_\alpha}} s} \right], \tag{2.12}$$

for the energy flow. A_α^+ and A_α^- are two arbitrary constants which have to be determined with appropriate boundary conditions usually expressed by I_α. It should be noticed that a similar equation governs each propagating wave. In fact, the wave uncoupling is assumed inside the bar. In fact, no wave energy transfer occurs far from the singularities. The wave coupling will be assumed to take place at the junctions and interfaces.

3. Coupling conditions for the energy equations

To close the energy description, boundary and coupling conditions as well as the second term needed for the differential equation must be discussed. Indeed, let us consider first a complex junction between a set of **m** waveguides. Each of them transmits a set of **n** kinds of propagating waves. From the previous

section, it follows that each kind of waves can be described by a second-order energy differential equation, so that a set of $(m * n)$ coupling conditions for energy parameters is required to close the problem. The most general form of those conditions is given below in a convenient computable way.

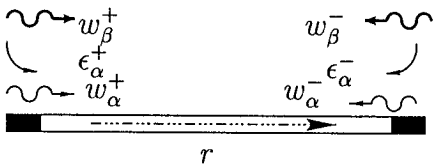

FIG. 2. Waves considered next

In the next subsections, the propagating waves sets will be denoted by $w_{\beta r}$, where β concerns waves of non-dispersive nature $(\mathbf{1} \leq \beta \leq \mathbf{n_1})$ (see Fig. 2), and where r is the waveguide index $(\mathbf{1} \leq \mathbf{r} \leq \mathbf{m})$. In addition, $w_{\alpha r}$ is the set of non-dispersive waves, $(\mathbf{1} \leq \alpha \leq \mathbf{n_2})$. Obviously, $n_1 + n_2 = n$ is the total number of waves to be considered. It should be eventually noticed that evanescent waves $\epsilon_{\alpha r}$, with $(\mathbf{1} \leq \alpha \leq \mathbf{n_2})$ are needed to describe correctly the waveguides interfaces.

3.1. Boundary and coupling conditions: unloaded singularity

At a junction, a set of propagating and evanescent waves exists. Those waves are divided into two parts. The first set comprises only propagating waves arriving to the interface. The vector containing such progressive waves is $\{w_e\}$. The second set of waves are those stemming from the junction. Those waves are in general of propagating and evanescent kind. The vector of waves arising of the interface is $\{w_o\}$. Using the convention adopted for the interface (Fig. 3), the defined vectors can be readily written as:

$$\{w_{\mathbf{e}}\} \overset{\text{def}}{=} \{w_{\delta \mathbf{r}}^+\}, \quad \{w_{\mathbf{o}}\} \overset{\text{def}}{=} \{w_{\delta \mathbf{r}}^-, \epsilon_\alpha\}. \tag{3.1}$$

δ denotes progressives waves of dispersive or non-dispersive nature. $\{w_e\}$ is a column of $n * m$ line number, whilst $\{w_o\}$ is a $(n + n_1) * m$ number of lines. The equilibrium and compatibility equations, when expressed at the junction, link this waves present at the interface. In the general case considered here, a set of $(2 * n_1 + n_2) * m$ equations is needed. Those relationships can be written, with regard to expression (3.1), as follows:

$$[\mathbf{E}]\{w_e\} = [\mathbf{S}]\{w_o\}. \tag{3.2}$$

$[\mathbf{E}]$ is a $n_{eq} * n_e$ matrix dimension, where $n_{eq} = (2 * n_1 + n_2) * m$ and $n_e = n * m$. $[\mathbf{S}]$ is a $n_o * n_o$ matrix dimension, where $n_o = (2 * n_1 + n_2) * m$. This relation (3.2)

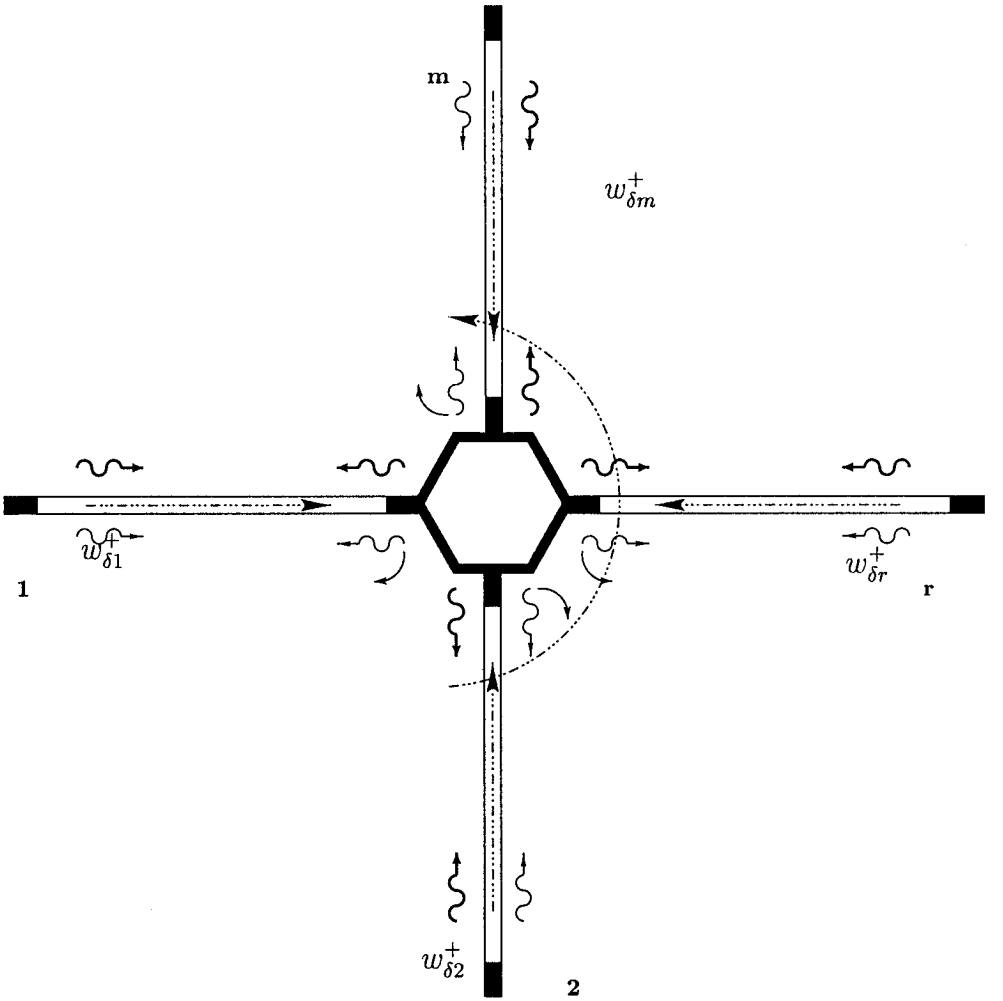

FIG. 3. Incident waves and reflected or transmitted waves at a junction

assimilates an interface to a wave converter with an input-output constitutive law. From this law (3.2), the waves arising from the interface can be deduced from the impinging ones simply by:

$$\{w_o\} = [\mathbf{S}]^{(-1)}\,[\mathbf{E}]\,\{w_e\}. \tag{3.3}$$

Thus, an interface will be completely described from the knowledge of matrix [**E**] and [**S**]. The resulting matrix (3.3) contains hence the reflection and transmission coefficients which represent the interface behavior from a wave description. It can be noticed that (3.3) is the exact formulation of the coupling conditions, and that the latter can be detailed as follows:

$$\left\{ \begin{array}{c} w^-_{\delta r} \\ \epsilon_{\alpha r} \end{array} \right\} = \left[\begin{array}{c} \mathbf{P} \\ \mathbf{Q} \end{array} \right] \{w^+_{\delta r}\}. \tag{3.4}$$

[**P**] is a $n_e * n_e$ matrix dimension, where $n_e = n * m$. [**Q**] is a $(n_1 * m) * (n * m)$ matrix. The coupling conditions suited for the energy equation described in the previous section are deduced from the propagating-propagating relationships at the junction. Hence, the useful relationship from (3.4) is:

$$\{w^-_{\delta r}\} = [\mathbf{P}]\,\{w^+_{\delta r}\}. \tag{3.5}$$

The quadratic form of this expression (3.5) can be readily deduced, expressing the modulus of each term in (3.5). Indeed, relationship (3.5) can be written as follows (3.6):

$$w^-_{\delta r} = \sum_{\gamma s=1}^{n*m} \mathbf{P}_{\delta \mathbf{r} \gamma \mathbf{s}} w^+_{\gamma s}. \tag{3.6}$$

Thus:

$$w^-_{\delta r} \times w^{*-}_{\delta r} = \sum_{\gamma s=1}^{n*m} \mathbf{P}_{\delta \mathbf{r} \gamma \mathbf{s}} \times \mathbf{P}^*_{\delta \mathbf{r} \gamma \mathbf{s}} w^+_{\gamma s} \times w^{*+}_{\gamma s} + \sum_{\gamma s=1}^{n*m} \sum_{\zeta t=1}^{n*m} \mathbf{P}_{\delta \mathbf{r} \gamma \mathbf{s}} \times \mathbf{P}^*_{\delta \mathbf{r} \zeta \mathbf{t}} w^+_{\gamma s} \times w^{*+}_{\zeta t}. \tag{3.7}$$

At this stage, the previous relationship can be simplified by omitting the second term in the equation. In fact, this term is the contribution of interferences to the partial energy associated to each wave. It has a space and frequency oscillating aspect which have been removed in the context of energy flow equation.

A number of publications and works in the literature discuss the validity of this simplification, the reader can obtain explanations from [16 – 19] and [20]. Thus:

$$w_{\delta r}^{-} \times w_{\delta r}^{*-} = \sum_{\gamma s=1}^{n*m} \mathbf{P}_{\delta \mathbf{r}\gamma \mathbf{s}} \times \mathbf{P}_{\delta \mathbf{r}\gamma \mathbf{s}}^{*} w_{\gamma s}^{+} \times w_{\gamma s}^{*+}. \tag{3.8}$$

Using this simplification and Eq. (2.1), one can obtain:

$$I_{\delta r}^{-} = \sum_{\gamma s=1}^{n*m} (Z_{\delta r}/Z_{\gamma s}) \times \mathbf{P}_{\delta \mathbf{r}\gamma \mathbf{s}} \times \mathbf{P}_{\delta \mathbf{r}\gamma \mathbf{s}}^{*} \times I_{\gamma s}^{+}. \tag{3.9}$$

This expression can be considered as the generalization of coupling conditions given by several authors, in particular, NEFSKE [3] and CHO in [21, 22]. Equation (3.10) represents a set of $(m * n)$ coupling conditions required to close the energy problem and to solve the differential equations. Note that those equations are written in terms of the partial energy quantities. A different version of these relationships is used in the section *Direct stiffness energy implementation.* Eventually, a general form of the reciprocity principle (consequence of the Maxwell-Betti theorem) can be formulated from Eq. (3.10) as follows:

$$\forall \gamma s, \qquad \sum_{\gamma s=1}^{n*m} (Z_{\delta r}/Z_{\gamma s}) \times \mathbf{P}_{\delta \mathbf{r}\gamma \mathbf{s}} \times \mathbf{P}_{\delta \mathbf{r}\gamma \mathbf{s}}^{*} = \mathbf{1}. \tag{3.10}$$

This expression is a generalization of the similar expression given by NEFSKE [3] and CHO [21].

3.2. Boundary and coupling conditions: loaded singularity

In this subsection, the treatment of an input force at a complex junction is considered. The procedure used below is similar to the one adopted before. Hencefore, propagative and evanescent waves are divided into: a vector of progressive waves entering the junction $\{w_e\}$, and a set of waves stemming from the junction $\{w_o\}$. Moreover, the vector $\{F\}$ contains concentrated external generalized forces (forces, moments,...) which are assumed to be known. The force vector is a column of n_f elements. Those parameters are linked to the entering waves quantities. For convenience following the convention adopted here (see Fig. 3), it follows:

$$\{w_e\} \overset{\text{def}}{\frown} \{w_{\sigma r}^{+}, F\}^{\mathrm{t}}, \qquad \{w_o\} \overset{\text{def}}{\frown} \{w_{\sigma r}^{-}, \epsilon_\alpha\}^{\mathrm{t}}. \tag{3.11}$$

Here, δ denotes progressive waves of dispersive or non-dispersive nature. $\{w_e\}$, is a column of $(n * m + n_f)$ lines, whilst $\{w_o\}$ is a column of $(n + n_1) * m$

lines. Equilibrium and compatibility equations expressed at the junction, link the defined vectors as follows:

$$[\mathbf{E}]\{w_e\} = [\mathbf{S}]\{w_o\}. \tag{3.12}$$

$[\mathbf{E}]$ is a $n_{eq} * n_e$ matrix , where $n_{eq} = (2 * n_1 + n_2) * m$ and $n_e = n * m + n_f$. $[\mathbf{S}]$ is a $n_o * n_o$ matrix , where $n_o = (2 * n_1 + n_2) * m$. From this law (3.12), the following expression can be deduced:

$$\{w_o\} = [\mathbf{S}]^{(-1)}[\mathbf{E}]\left\{w_{\delta r}^{+}, F\right\}^{\mathbf{t}}. \tag{3.13}$$

Thus, the loaded interface will be completely described from the knowledge of matrix $[\mathbf{E}]$ and $[\mathbf{S}]$ and the force vector $\{F\}$. In fact:

$$\begin{Bmatrix} w_{\alpha r}^{-} \\ \epsilon_{\alpha r} \end{Bmatrix} = \begin{bmatrix} \mathbf{P} & \mathbf{R} \\ \mathbf{Q} & \mathbf{S} \end{bmatrix} \left\{w_{\delta r}^{+}, F\right\}^{t}. \tag{3.14}$$

and:

$$w_{\delta r}^{-} = \sum_{\gamma s=1}^{n*m} \mathbf{P}_{\delta \mathbf{r}\gamma \mathbf{s}} w_{\gamma s}^{+} + \sum_{t=1}^{n_f} \mathbf{R}_{\delta \mathbf{r}t} F_{\delta rt}. \tag{3.15}$$

The quadratic form of this expression (3.15) can be readily deduced by expressing the modulus of the wave arising from the junction, as a function of incident waves and input forces:

$$w_{\alpha r}^{-} \times w_{\alpha r}^{*-} = \Sigma_1 + \Sigma_2 + \Sigma_3. \tag{3.16}$$

where:

$$\Sigma_1 = \sum_{\gamma s=1}^{n*m} \mathbf{P}^{\mathbf{2}}_{\gamma \mathbf{s}\delta \mathbf{r}} w_{\gamma s}^{+} \times w_{\beta s}^{*+} + \sum_{t=1}^{n_f} \mathbf{R}^{\mathbf{2}}_{\delta \mathbf{r}t} F^{2}_{\delta rt}. \tag{3.17}$$

$$\Sigma_2 = \sum_{\gamma s=1}^{n*m} \sum_{\substack{\zeta t=1 \\ \zeta t \neq \gamma s}}^{n*m} \mathbf{P}_{\gamma \mathbf{s}\delta \mathbf{r}} \mathbf{P}^{*}_{\zeta \mathbf{t}\delta \mathbf{r}} w_{\delta r}^{+} \times w_{\zeta t}^{*+} + \sum_{t=1}^{n_f} \sum_{\substack{k=1 \\ k \neq t}}^{n_f} \mathbf{R}_{\delta \mathbf{r}t} \mathbf{R}^{*}_{\delta \mathbf{r}k} F_{\delta rt} F^{*}_{\delta rk}. \tag{3.18}$$

$$\Sigma_3 = \sum_{\gamma s=1}^{n*m} \sum_{t=1}^{n_f} \mathbf{P}_{\gamma \mathbf{s}\delta \mathbf{r}} \mathbf{R}^{*}_{\delta \mathbf{r}t} w_{\gamma s}^{+} \times F_{\beta s}^{*+} + \sum_{\gamma s=1}^{n*m} \sum_{t=1}^{n_f} \mathbf{P}^{*}_{\gamma \mathbf{s}\delta \mathbf{r}} \mathbf{R}_{\delta \mathbf{r}t} w_{\gamma s}^{*+} \times F_{\beta s}^{+}. \tag{3.19}$$

Therefore, assuming that no correlation exists between the different sources occurring in this problem (this means that the external input sources and the

arising waves are not correlated), this is a high frequency consequence which has been addressed by some authors (see for instance [23, 24]), the previous relationship can be simplified by omitting terms in the Equation (3.16), the contribution of (3.18) and (3.19).

$$w^{-}_{\alpha r} \times w^{*-}_{\alpha r} = \sum_{\gamma s=1}^{n*m} \mathbf{P}^{2}_{\gamma s \delta r} w^{+}_{\gamma s} \times w^{*+}_{\beta s} + \sum_{t=1}^{n_f} \mathbf{R}^{2}_{\delta r t} F^{2}_{\delta r t}. \tag{3.20}$$

which leads finally to:

$$I^{-}_{\delta r} = \sum_{\gamma s=1}^{n*m} (Z_{\delta r}/Z_{\gamma s}) \times \mathbf{P}_{\delta r \gamma s} \times \mathbf{P}^{*}_{\delta r \gamma s} \times I^{+}_{\gamma s} + \sum_{t=1}^{n_f} Z_{\delta r} \mathbf{R}^{2}_{\delta r t} F^{2}_{\delta r t}. \tag{3.21}$$

Equation (3.21) represents the set of $(m * n)$ of coupling conditions required to close the energy problem and to solve the differential equations.

4. Direct stiffness energy based implementation

In this section the numerical method used to solve the energy equations is dealt with. The direct stiffness method [25] is fitted to the energy equations. It has been used and implemented for a number of dynamical cases and especially for waveguides, particular plates coupling, etc. (see [25]). Its major feature consists in giving the "exact" solution of the dynamical behavior of complex structures, whereas finite element implementation for instance requires a set of approximations.

4.1. Elementary energy transfert matrix for complex one dimensional

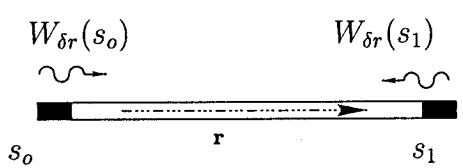

Fig. 4. Elementary energy wave guide, nodal parameters

Let us consider first the simplest waveguide with a unique travelling wave. Fig. 4 presents the sign convention used here. Each element is defined by two nodes where the energy parameters are assumed to be unknown. Thus, the purpose of the following process is to express the transfer between nodes with regard

to the energy equation discussed in Sec. 1. To this end, let us recall the general particular solution of the energy equation:

$$W_{\delta r}(s) = A^{+}_{\delta r} e^{-\frac{\eta_{\delta r}\omega}{c_{g_{\delta r}}}s} + A^{-}_{\delta r} e^{\frac{\eta_{\delta r}\omega}{c_{g_{\delta r}}}s}, \tag{4.1}$$

for the energy density, and:

$$I_{\delta r}(s) = c_{g_{\delta r}} \left[A^{+}_{\delta r} e^{-\frac{\eta_{\delta r}\omega}{c_{g_{\delta r}}}s} - A^{-}_{\delta r} e^{\frac{\eta_{\delta r}\omega}{c_{g_{\delta r}}}s} \right], \tag{4.2}$$

for the energy flow. Let us now define an energy density vector and an active energy vector, so that:

$$\{W_{\delta r}\} = \begin{pmatrix} W_{\delta r}(s_o) \\ W_{\delta r}(s_1) \end{pmatrix}, \tag{4.3}$$

for the energy density, and:

$$\{I_{\delta r}\} = \begin{pmatrix} I_{\delta r}(s_o) \\ -I_{\delta r}(s_1) \end{pmatrix}, \tag{4.4}$$

for the energy flow. Expressing now the energy density vector on the abscissa corresponding to nodes 1 and 2 and using the explicit form giving (4.1) and (4.2), it follows:

$$\{W_{\delta r}\} = \begin{bmatrix} e^{\frac{-\eta\omega}{c_{g_{\delta r}}}s_0} & e^{\frac{\eta\omega}{c_{g_{\delta r}}}s_0} \\ e^{\frac{-\eta\omega}{c_{g_{\delta r}}}s_1} & e^{\frac{\eta\omega}{c_{g_{\delta r}}}s_1} \end{bmatrix} \begin{pmatrix} A^{+}_{\delta r} \\ A^{-}_{\delta r} \end{pmatrix}, \tag{4.5}$$

for the energy density, and:

$$\{I_{\delta r}\} = c_{g_{\delta r}} \begin{bmatrix} e^{\frac{-\eta\omega}{c_{g_{\delta r}}}s_0} & -e^{\frac{\eta\omega}{c_{g_{\delta r}}}s_0} \\ -e^{\frac{-\eta\omega}{c_{g_{\delta r}}}s_1} & e^{\frac{\eta\omega}{c_{g_{\delta r}}}s_1} \end{bmatrix} \begin{pmatrix} A^{+}_{\delta r} \\ A^{-}_{\delta r} \end{pmatrix}, \tag{4.6}$$

for the energy flow vector. Eliminating amplitudes $A^{+}_{\delta r}$ and $A^{-}_{\delta r}$ from (4.6) and (4.5), the energy-equivalent "stiffness" operator can be presented:

$$\{I_{\delta r}\} = \frac{c_{g_{\delta r}}}{\sinh\left(\frac{\eta\omega}{c_{g_{\delta r}}}l_r\right)} \begin{bmatrix} \cosh\left(\frac{\eta\omega}{c_{g_{\delta r}}}l_r\right) & -1 \\ -1 & \cosh\left(\frac{\eta\omega}{c_{g_{\delta r}}}l_r\right) \end{bmatrix} \{W_{\delta r}\}. \tag{4.7}$$

or simply:

$$\{I_{\delta r}\} = [\mathbf{K}_{\delta \mathbf{r}}]\{W_{\delta r}\}, \tag{4.8}$$

where $l_r = (s_1 - s_o)$ is the "r-th" element length. $[\mathbf{K}_{\delta \mathbf{r}}]$ denotes an energy operator equivalent to the classical kinematic "stiffness". This matrix is symmetric which prove the reciprocity of the energy equation. For the single element case given in Fig. 4, the matrix formulation of the problem is completely determined from the knowledge of the boundary condition expressed in terms of the active energy flow as well as the power input in the system.

4.2. Elementary energy matrix assembly

As in the classical finite element method, elementary matrix must be assembled, in order to deal with complex geometry and configuration. The displacement finite element procedure is well established and easy to implement according mainly to the compatibility of shape functions. The displacement continuity and forces equilibrium are simply included. However, such a generalization cannot be envisaged when speaking about energy equations. Indeed, as it was seen in the previous sections, energy coupling conditions are not easy do deal with, specially, when complex waveguide interface is considered. The assembly procedure used here, is similar to the one presented in [21]. It will be generalized for a numerical implementation scheme. Indeed in the following, the interface involving an energy gap will be regarded as an *intrinsic element.* The dimension of this element will depend on the complexity of the interface. So, let us recall the energy coupling conditions established before:

$$I_{\delta r}^{-} = \sum_{\gamma s=1}^{n*m} (Z_{\delta r}/Z_{\gamma s}) \times \mathbf{P}_{\delta \mathbf{r} \gamma \mathbf{s}} \times \mathbf{P}_{\delta \mathbf{r} \gamma \mathbf{s}}^{*} \times I_{\gamma s}^{+} + \sum_{t=1}^{n_f} Z_{\delta r} \mathbf{R}_{\delta \mathbf{r} \mathbf{t}}^{\mathbf{2}} F_{\delta r t}^{2}. \tag{4.9}$$

This relationship is expressed in terms of partial active energy associated with different wave forms. In order to establish the general expression of the matrix representing the interface behavior in terms of energy density and active energy flow, the formula (4.9) must be rewritten. Indeed, from Eqs. (2.11) and (4.2), partial energies associated with a wave of kind α can be obtained from global energies thanks to nothing else but the total energy density $W(s)$ (2.2):

$$I_{\delta r}^{+} = \frac{1}{2} (I_{\delta r} + c_{g_{\delta r}} W_{\delta r}), \tag{4.10}$$

on the one hand, and:

$$I_{\delta r}^{-} = \frac{1}{2} (I_{\delta r} - c_{g_{\delta r}} W_{\delta r}), \tag{4.11}$$

on the other hand. Those relationships are valid for each partial energy appearing in (4.9). Hence, combining the latter with (4.10) and (4.11), one can obtain a

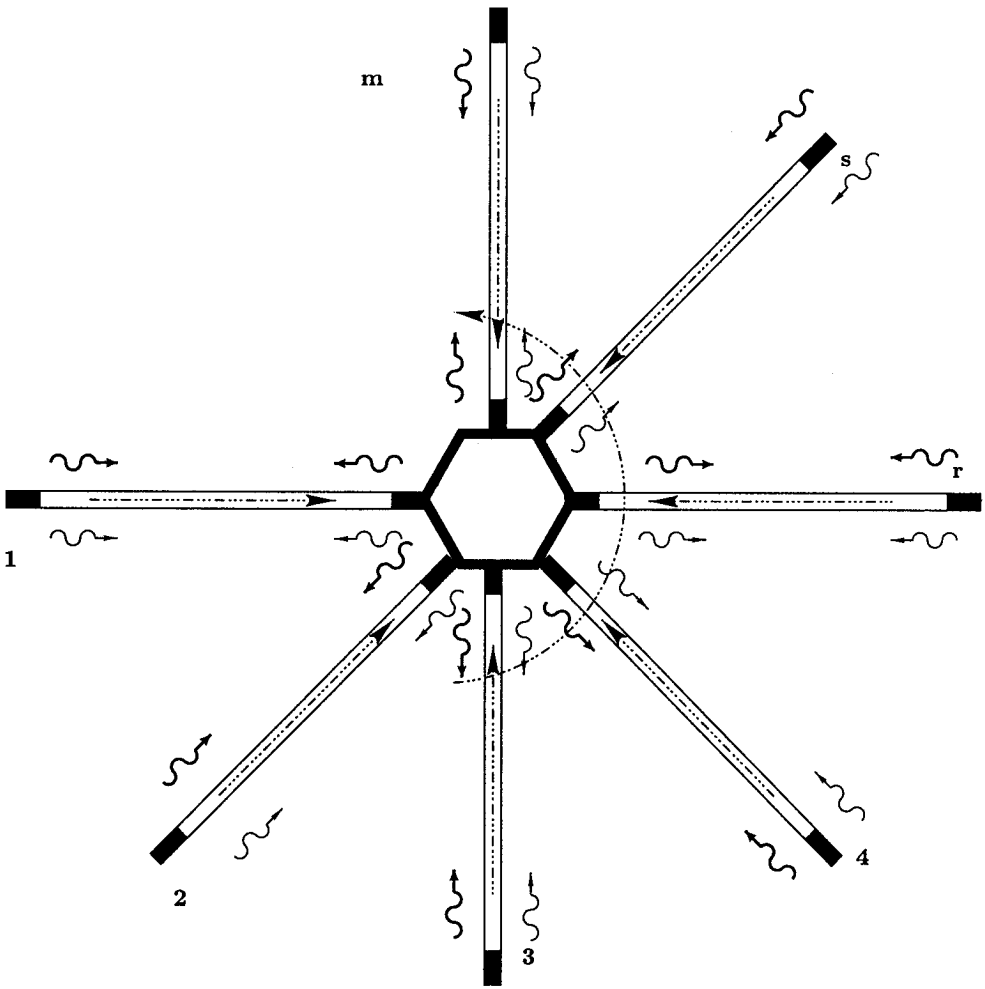

FIG. 5. Complex wave guide interface energy treatments

new form of (4.9) after some calculations:

$$(4.12)\quad \sum_{\gamma s}^{n*m}(\mathbf{1}_{\gamma s\delta r}-\Delta_{\gamma s\delta r})I_{\gamma s}=\sum_{\gamma s}^{n*m}(c_{g_{\delta r}}\mathbf{1}_{\gamma s\delta r}+\Delta_{\gamma s\delta r})\,W_{\gamma s}+\sum_{t=1}^{n_f}Z_{\delta r}\,\mathbf{R}^2_{\delta rt}F^2_{\delta rt},$$

where:

$$(4.13)\quad \Delta_{\gamma s\delta r}=(Z_{\delta r}/Z_{\gamma s})\times\mathbf{P}_{\delta r\gamma s}\times\mathbf{P}^*_{\delta r\gamma s},$$

$$(4.14)\quad \begin{aligned}\mathbf{1}_{\gamma s\delta r}&=\mathbf{1}\quad\text{if}\quad \gamma s=\delta r,\\ \mathbf{1}_{\gamma s\delta r}&=\mathbf{0}\quad\text{if}\quad \gamma s\neq\delta r.\end{aligned}$$

This is the general form of the interface description according to the energy equation formulation. The interface matrix dimension depends on the number of waveguides present at the connection, and on the number of waves considered in each waveguide.

$$(4.15)\quad ([\mathbf{1}_{\gamma s\delta r}]-[\Delta_{\gamma s\delta r}])\{I_{\gamma s}\}=([c_{g_{\delta r}}\mathbf{1}_{\gamma s\delta r}]+c_{g_{\gamma s}}[\Delta_{\gamma s\delta r}])\{W_{\gamma s}\}+\{H_{\gamma s}\}\{F^2_{\delta rt}\}.$$

It should be noted that the resulting matrix contains the reflection and transmission efficiencies of the considered interface.

$$(4.16)\quad \{I_{\gamma s}\}=([\mathbf{1}_{\gamma s\delta r}]-[\Delta_{\gamma s\delta r}])^{-1}([c_{g_{\delta r}}\mathbf{1}_{\gamma s\delta r}]+c_{g_{\gamma s}}[\Delta_{\gamma s\delta r}])\{W_{\gamma s}\}+([\mathbf{1}_{\gamma s\delta r}]-[\Delta_{\gamma s\delta r}])^{-1}\{H_{\gamma s}\}\{F^2_{\delta rt}\}.$$

In the case of a unloaded region, this expression leads to:

$$(4.17)\quad \{I_{\gamma s}\}=([\mathbf{1}_{\gamma s\delta r}]-[\Delta_{\gamma s\delta r}])^{-1}([c_{g_{\delta r}}\mathbf{1}_{\gamma s\delta r}]+c_{g_{\gamma s}}[\Delta_{\gamma s\delta r}])\{W_{\gamma s}\}.$$

Henceforth:

$$(4.18)\quad \{I_{\gamma s}\}=[\mathbf{Z}_{\gamma s}]\,\{W_{\gamma s}\}.$$

Actually, the intrinsic form of the interface treatment in the energy formulation will induce a special treatment of the assembling procedure, where finally, the interface will be regarded as a complex element of variable dimension. The latter is computed in the general case.

4.3. Energy-based code

In this section, the implementation of the numerical energy is briefly explained. In particular, the subtleties induced by the energy features are discussed.

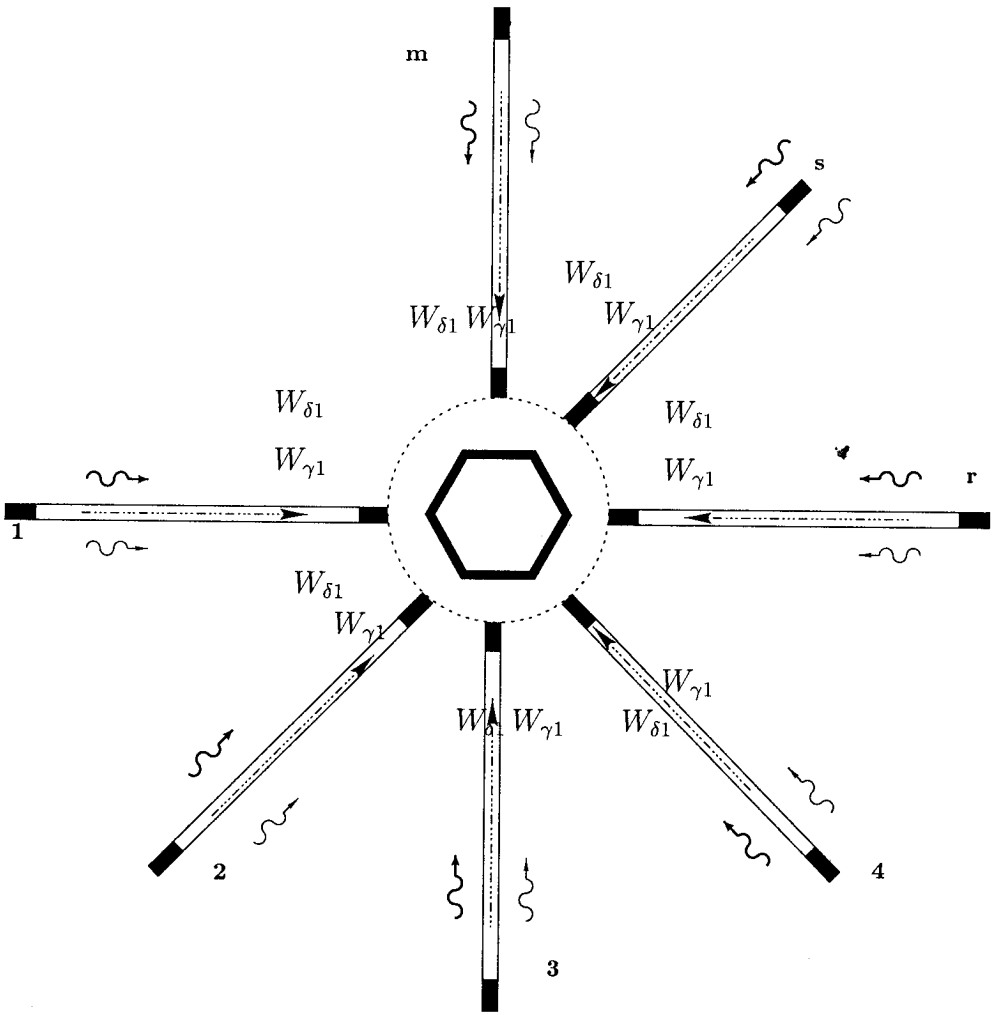

FIG. 6. Nodal energy unknown variables at the interface

Indeed, the non-trivial form of the coupling conditions treatment requires careful attention in the numerical computation of the technique. As shown before, the resulting global energy stiffness matrix will not be in general symmetric. However, special attention paid to the correspondence between global and local nodal numbering, can make this matrix nearly band. To this end, the best way is to implement a numbering procedure, which takes into account the interface behavior in the energy description.

5. Complex structure validation

Let us now consider a numerical complex test in order to validate the computed method. It should be noted that the concerned structure is extracted from a submarine construction. Furthermore, this structure has been studied as a "benchmark" test for the structural path analysis proposed by Girard [13]. This structure has been studied also by Bondoux in the context of the implementation of a ray theory analysis [14]. Figure 7 presents the studied structure. It is a plane truss composed of twenty four wave guides. In the following, extensional and flexural waves have been taken into account in the energy computation. The interest of this structure remains in the relative complexity of the existing interfaces between waveguides. Figure 7 shows also the node numbering. The excitation is assumed to be on node 3. Characteristics of the structure are summarized in Table 1. The waveguides are assumed to be of identical cross-sections. A constant damping ratio of 0.04 is assumed and introduced next. The component lengths are directly reported in Fig. 7. As only two waves are dealt with

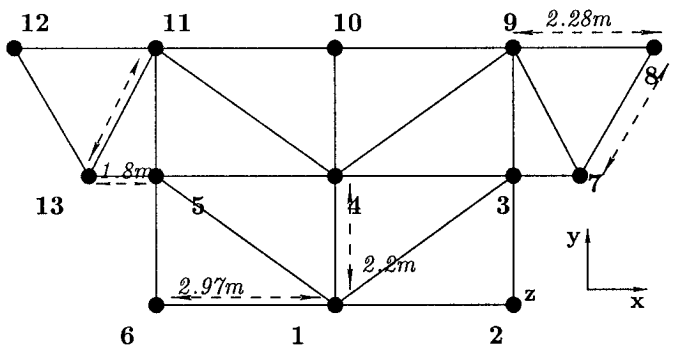

Fig. 7. The studied 24 components beam-like structure

here, an energy model of 96 energetic degrees of freedom is needed. Indeed, each of the 24 waveguides is represented by 4 energy unknowns.

Table 1. The beam truss components mechanical and geometrical characteristics.

	Inertia (m^4)	Section (m^2)	η %	Density Kg m^{-3}	Young mod. (P_a)
All beams	5.34×10^{-5}	9.024×10^{-3}	4	7700	2×10^{11}

5.1. The geometry of the validation test

The energy numbering technique of the energy unknown is proposed in Fig. 9. It makes easy the implementation of the energy method with regard to the interface complexity. Figure 8 gives a picture of the resulting global energy matrix, and confirms the fact that this matrix is neither symmetric nor a band matrix. However, the numerical gain obtained from the energy equation up to high frequencies, remains important and compensates the loss of symmetry of the resulting energy matrix.

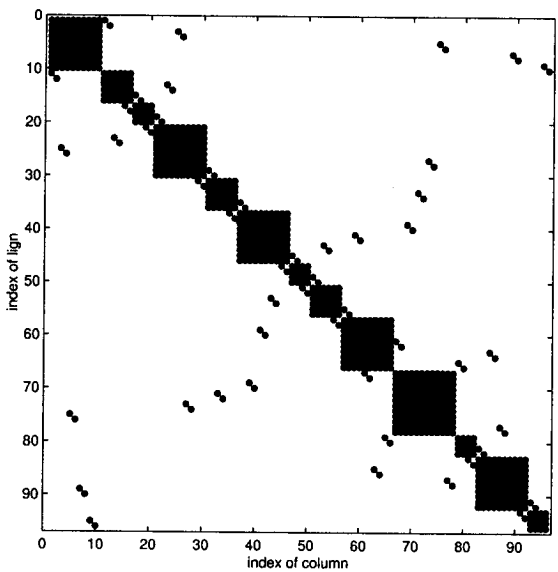

FIG. 8. Picture of the energy stiffness matrix.

5.2. The reference results

In order to compare to the energy results, a finite element analysis of the plane structure has been performed. This calculation used here as reference results will be considered as the "exact" computation of the truss response. Typical results obtained from this computation is given in Fig. 11, which present the longitudinal velocity of point 12 when a horizontal excitation is assumed. It should be noted

that this response is dominated by the modal behavior of the truss and that up to 10 kHz, a great number of modes are required in order to compute the solution.

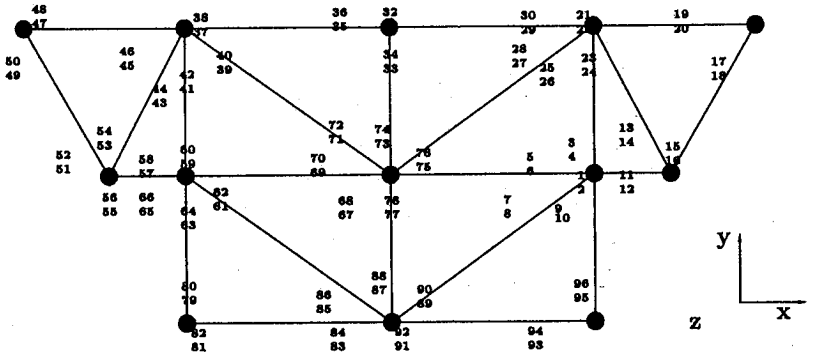

FIG. 9. Nodal energy numbering in view of the method implementation.

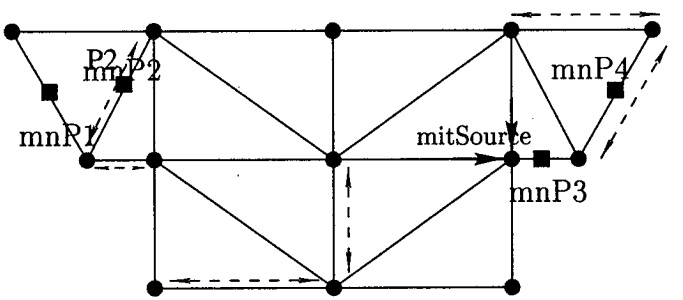

FIG. 10. Input forces key points and output results location.

5.3. Comparison for flexural excitation at point 3

Let us introduce a vertical force (with respect to the y-axis) on the point 3. This is a transversal force of $1N$ amplitude. Figures 11-15 give an outline of energy computations. Actually, the energy results given, prove that the energy equation gives a direct prediction of mean values of the expected dynamical levels. Indeed, the energy equation, smooths the response and gives, at a low computational cost, an average prediction of the expected results. Therefore, the energy equation computation requires a very limited frequency sampling and spatial meshing of the structure.

Furthermore, as suggested by the authors in [9], an envelope estimation of the prediction can be performed from the energy equation predictions.

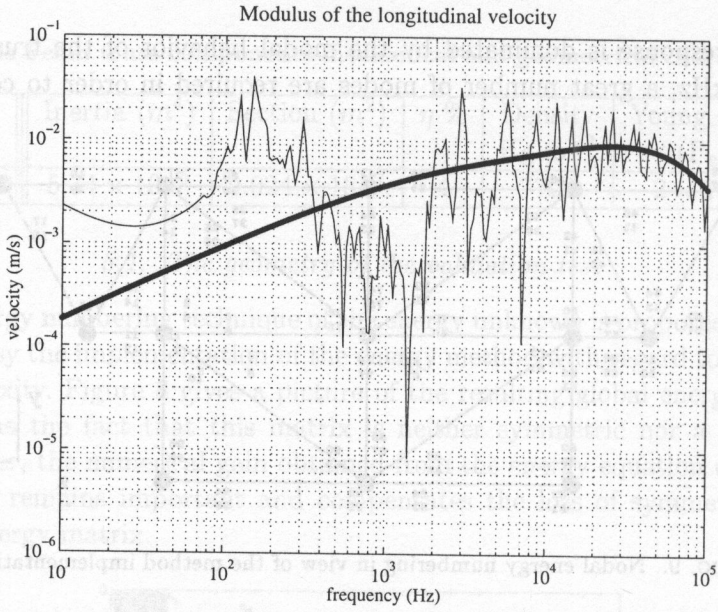

FIG. 11. Modulus of the longitudinal velocity at the middle of bar 3-7 (Point P3): comparison between energy code results and the reference calculation.

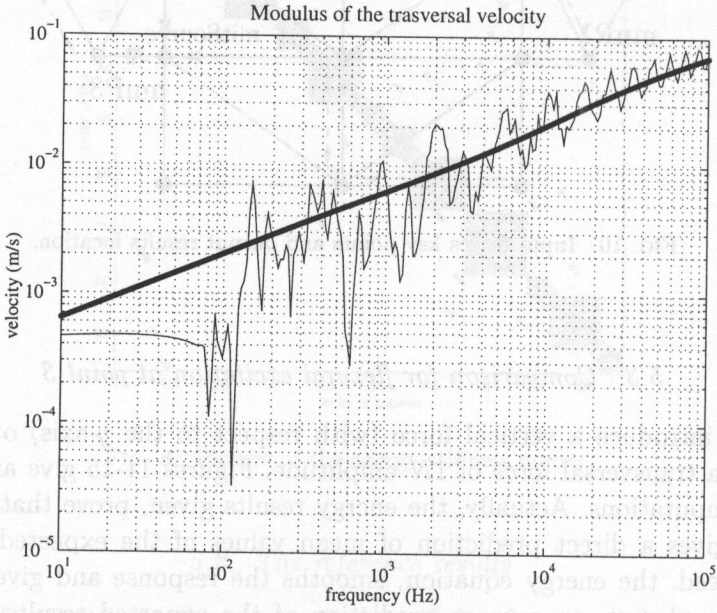

FIG. 12. Modulus of the transversal velocity at point at the middle of bar 3-7 (Point P3): comparison between energy code results and the reference calculation.

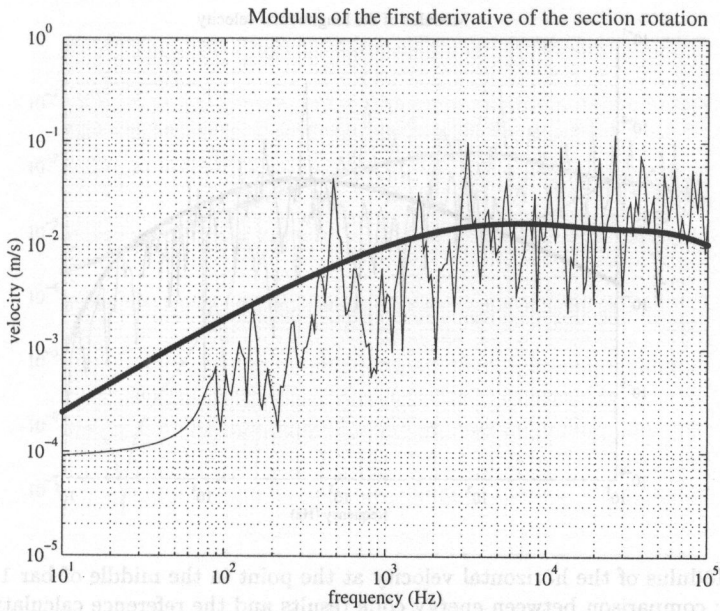

FIG. 13. Modulus of the slope velocity at the middle of bar 11-13 (Point P2): comparison between energy code results and the reference calculation.

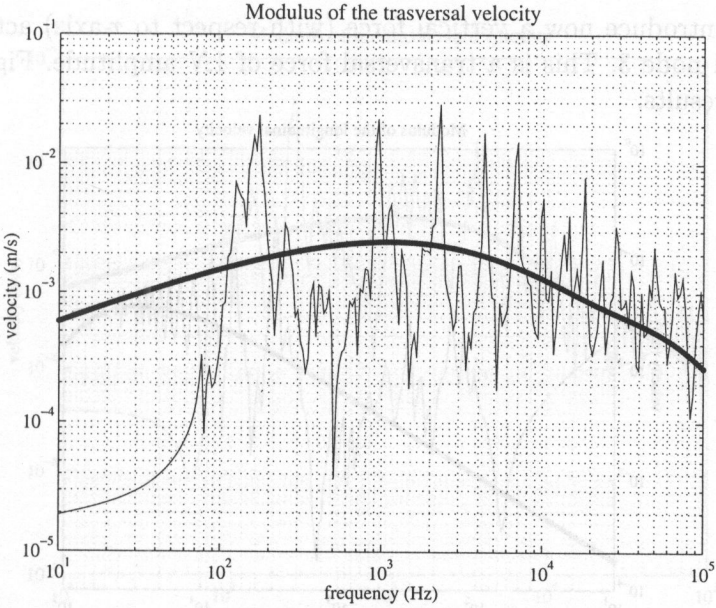

FIG. 14. Modulus of the transversal velocity at the middle of bar 11-13 (Point P2): comparison between energy code results and the reference calculation.

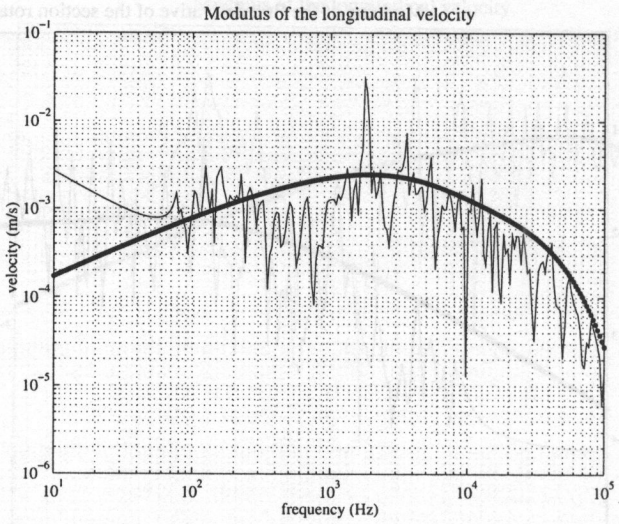

FIG. 15. Modulus of the horizontal velocity at the point in the middle of bar 11-13 (Point P2): comparison between energy code results and the reference calculation.

5.4. Comparison for extensional excitation at point 3

Let us introduce now a vertical force (with respect to x-axis) acting on the geometrical node 3. This is a transversal force of $1N$ amplitude. Figures 16-20 give some results.

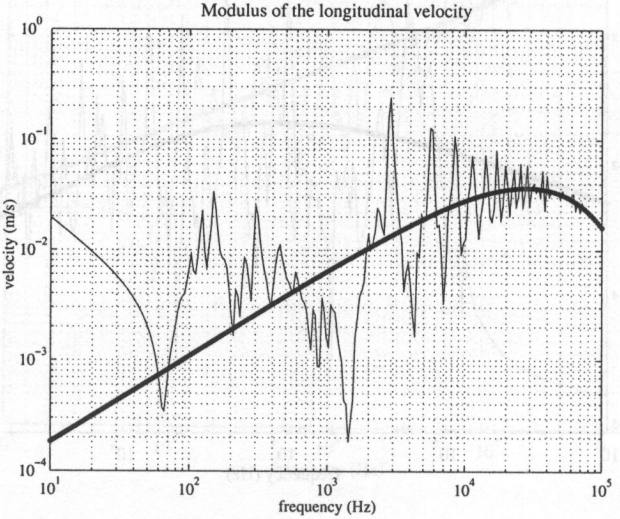

FIG. 16. Modulus of the transversal slope velocity at the middle of bar 12-13 (Point P1): comparison between energy code results and the reference calculation.

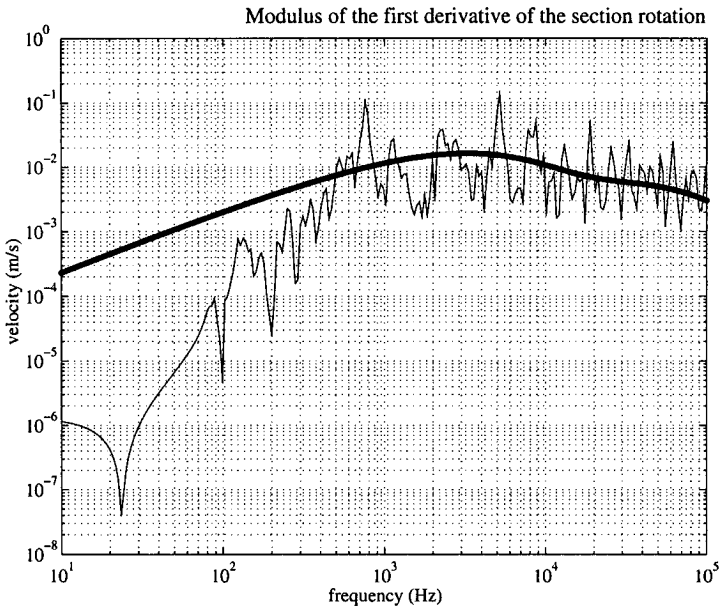

FIG. 17. Modulus of the transversal velocity at the middle of bar 12-13 (Point P1): comparison between energy code results and the reference calculation.

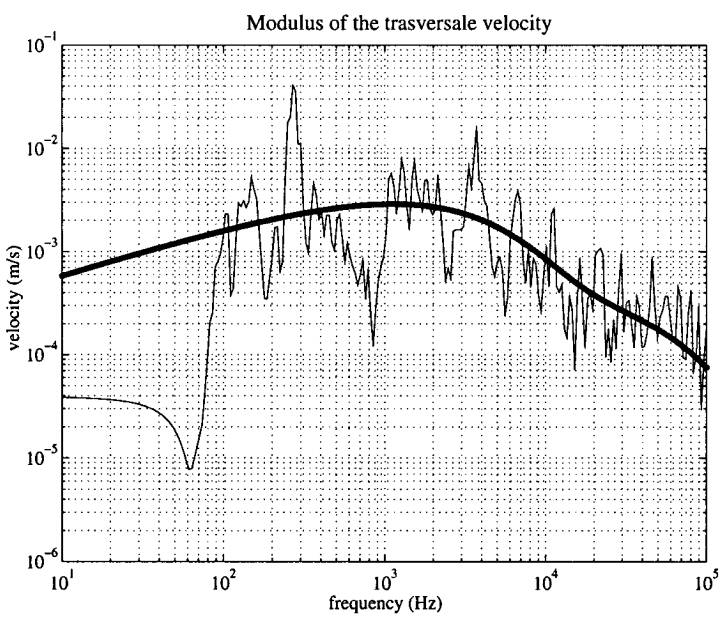

FIG. 18. Modulus of the transversal velocity at the middle of bar 7-8 (Point P4): comparison between energy code results and the reference calculation.

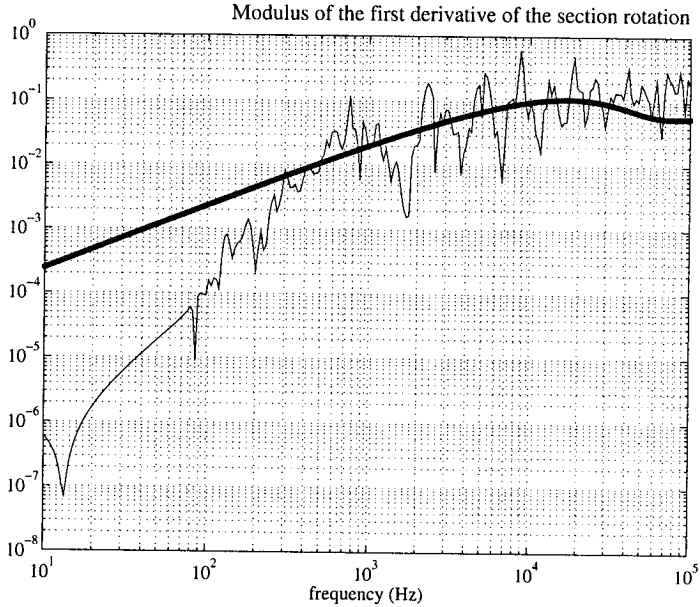

FIG. 19. Modulus of the transversal velocity in the middle of bar 7-8 (Point P4): comparison between energy code results and the reference calculation.

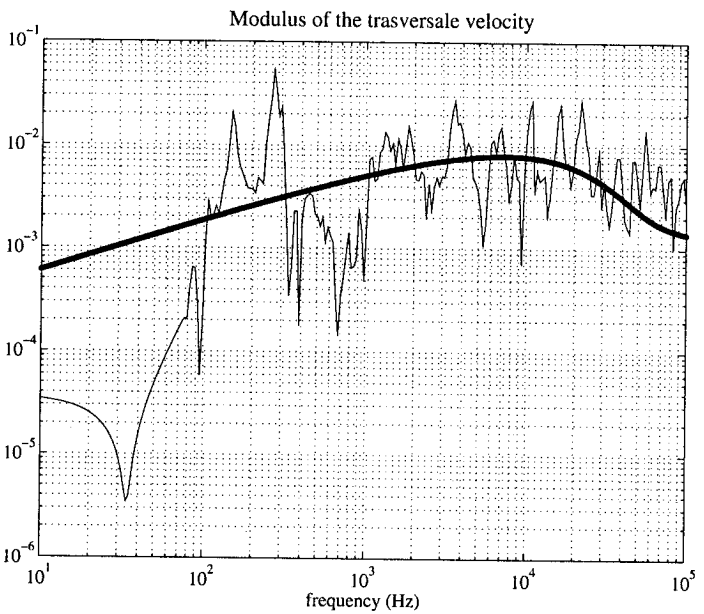

FIG. 20. Modulus of the transversal velocity in the middle of bar 3-7 (Point P3): comparison between energy code results and the reference calculation.

6. Conclusion

In this paper, the high frequency dynamics of a one-dimensional complex system has been analyzed by means of an energy equation. The basic formulation of the energy equation has been given first. It has been shown that the energy equation is based upon an energy superposition principle, which follows from neglecting the interferences in the wave description of the problem. This leads to an equation which gives smooth energy prediction. This formulation is thus well suited to deal with medium and high frequencies as it requires only a low computation cost, in comparison to the finite element modelling using classical formulation.

In view of a numerical implementation of the resulting equation, the coupling phenomenon related to this equation has been formulated. It has been shown that the energy boundary and coupling conditions can be formulated, in the most general case, by defining an interface input-output operator which describes completely the local behavior of waves. Finally, a numerical scheme able to take into account the energy equation features has been discussed.

The results obtained when testing a complex 24 component truss, show the ability of a developed formulation to predict the mean energy value of a one-dimensional complex system up to high frequency. This leads to an interesting tool which can help to design structures in a wide frequency band.

Acknowledgements

The author gratefully acknowledges Mr R. Aquilina (CERDAN TOULON) for his scientific collaboration, his advices and encouragements.

References

1. F. J. Fahy, *L'analyse statistique énergétique*, Revue d'Acoustique, **33**, 10-25, 1975.
2. S. A. Rybak, V. D. Belov, and B. D. Tartakovskii, *Propagation of vibrational energy in absorbing structures*, Soviet Physical Acoustic, **23**, 115-119, 1977.
3. D. J. Nefske and S. H. Sung, *Power flow finite element analysis of dynamic systems: basic theory and application to beams*, NCA Publication, **3**, 1987.
4. J. C. Wohlever and R. J. Bernhard, *Mechanical energy flow models of rods and beams*, Journal of Sound and Vibration, **153**, 1-19, 1992.
5. R. J. Bernhard, O. Bouthier and J. C. Wohlever, *Energy and structural intensity formulations of beam and plate vibrations*, 3rd International Congress on Intensity, Senlis, France, 1990.
6. O. M. Bouthier and R. J. Bernhard, *Simple models of energy flow in vibrating membranes*, Journal of Sound and Vibration, **182**, 129-147, 1995.
7. O. M. Bouthier and R. J. Bernhard, *Simple models of energy flow in vibrating plates*, Journal of Sound and Vibration, **182**, 149-164, 1995.
8. M. N. Ichchou, A. Le Bot and L. Jezequel, *Energy models of one-dimensional multi-propagative systems*, Journal of Sound and Vibration, **201**, 535-554, 1997.

9. A. LE BOT, M. N. ICHCHOU and L. JEZEQUEL, *Energy flow analysis for curved beams*, Journal of the Acoustical Society of America, **102**, 943-954, 1997.
10. M. N. ICHCHOU, A. LE BOT and L. JEZEQUEL, *Radial and tangential energy flow models for curved wave guides*, Vibration and Noise 95, 718-727, Venice, Italy, 1995.
11. M. N. ICHCHOU, A. LE BOT and L. JEZEQUEL, *Beam network analysis by a power flow method*, Transaction of ASME conference 95, 823-827, USA, Boston 1995.
12. Y. LASE, M. N. ICHCHOU and L. JEZEQUEL, *Energy analysis of bars an beams: theoretical formulations*, Journal of Sound and Vibration, **192**, 281-305, 1996.
13. A. GIRARD and DEFOSSE, *Frequency response smoothing, matrix assembly and structural paths: a new approach for structural dynamics up to high frequencies*, Journal of Sound and Vibration, **137**, 53-68, 1990.
14. R. AQUILINA, D. BONDOUX, and J. M. PAROT, *Structural broad band fields in beam networks by a vibratory rays model*, 3rd International Congress on Intensity, 85-94, Senlis, France, 1990.
15. L. BRILLOUIN, *Wave propagation in periodic structures*, Dover Publications, Inc., New York 1953.
16. M. DJIMADOUM and J. L. GUYADER, *Possibilities to generalize the heat transfer approach to vibration of plates problems*, Inter-Noise '95, CA, Newport Beach 1995.
17. B. R. MACE, *On the statistical energy analysis hypothesis of coupling power proportionality and some implications of its failure*, Journal of Sound and Vibration, **178**, 95-112, 1994.
18. R. S. LANGLEY, *Analysis of beam and plate vibrations by using the wave equation*, Journal of Sound and Vibration, **150**, 47-65, 1991.
19. R. S. LANGLEY, *A wave intensity technique for the analysis of high frequency vibrations*, Journal of Sound and Vibration, **159**, 483-502, 1992.
20. R. S. LANGLEY, *On the vibrational conductivity approach to high frequency dynamics for two-dimensional structural components*, Journal of Sound and Vibration, **182**, 637-657, 1995.
21. P. E. CHO, *Energy flow analysis of coupled structures*, Purdue University, PHD thesis, 1993.
22. P. E. CHO and R. J. BERNHARD, *A simple method for predicting the energy flow distributions in frame structures*, 3rd International Congress on Intensity, 347-354, Senlis, France 1990.
23. B. R. MACE, *Power flow between two continuous one-dimensional subsystems: a wave solution*, Journal of Sound and Vibration, **154**, 289-319, 1992.
24. B. R. MACE, *Power flow between two coupled beams*, Journal of Sound and Vibration, **159**, 305-325, 1992.
25. R. S. LANGLEY, *Application of the dynamic stiffnes method to the free and forced vibrations of aircraft panels*, Journal of Sound and Vibration, **135**, 319-339, 1989.

Received February 21, 2000.